



Finite-size effects on the convergence time in continuous-opinion dynamicsHang-Hyun Jo ^{1,*} and Naoki Masuda ^{2,3}¹*Department of Physics, The Catholic University of Korea, Bucheon 14662, Republic of Korea*²*Department of Mathematics, State University of New York at Buffalo, Buffalo, New York 14260-2900, USA*³*Computational and Data-Enabled Science and Engineering Program, State University of New York at Buffalo, Buffalo, New York 14260-5030, USA*

(Received 10 March 2021; accepted 25 June 2021; published 19 July 2021)

We study finite-size effects on the convergence time in a continuous-opinion dynamics model. In the model, each individual's opinion is represented by a real number on a finite interval, e.g., $[0,1]$, and a uniformly randomly chosen individual updates its opinion by partially mimicking the opinion of a uniformly randomly chosen neighbor. We numerically find that the characteristic time to the convergence increases as the system size increases according to a particular functional form in the case of lattice networks. In contrast, unless the individuals perfectly copy the opinion of their neighbors in each opinion updating, the convergence time is approximately independent of the system size in the case of regular random graphs, uncorrelated scale-free networks, and complete graphs. We also provide a mean-field analysis of the model to understand the case of the complete graph.

DOI: [10.1103/PhysRevE.104.014309](https://doi.org/10.1103/PhysRevE.104.014309)**I. INTRODUCTION**

In the last few decades, social dynamics has been extensively studied in various research fields including statistical physics and complex systems [1,2]. A main drive underlying such studies is that many social phenomena may be understood in terms of complex macroscopic patterns that emerge from the interaction between microscopic constituents. In the present study, we focus on opinion dynamics models, which have contributed to understanding how collective opinion evolves in a society of individuals who learn from their neighbors as well as from other sources of information such as media [1–9]. In these models, the structure of interaction among individuals has mainly been modeled by graphs, equivalently networks, in which nodes and edges represent individuals and their pairwise interaction, respectively [10–13].

Most models of opinion dynamics have assumed that the opinion of each individual is either a discrete or continuous variable. The prototypical model with discrete opinions is the voter model in which each individual takes one of the two opinions at any given time [14–17]. Multistate voter models are variants of the voter model in which individuals take one of more than two opinions [18–21]. Other variants include multistate opinion dynamics coevolving with the network structure [22–25] and multistate majority-vote models [26–31]. Opinion dynamics models with continuous opinions may be defined with or without bounded confidence [1,32–34]. Models with bounded confidence, such as the Deffuant-Weisbuch model [32] and the Hegselmann-Krause model [33], assume that individuals interact with each other only when their opinions are close enough. Continuous-

opinion models without the bounded confidence, which we consider in the present study, include the model by Abelson [35], the DeGroot model [36], the Friedkin-Johnsen model [37], and their variants. A majority of opinion dynamics models explored in control theory research community are continuous-opinion models as well [38–41].

A main concern in opinion dynamics models is the emergence of opinion clusters through agreement, compromise, or imitation processes, starting from initially random or diverse opinions [1–9]. When there is a unique opinion cluster in the stationarity, it is called the consensus. In the consensus, all individuals share the same opinion. The time needed to reach the consensus, i.e., the consensus time, is known to depend on the system size, i.e., the number of individuals. Relationships between the consensus time and the system size have been studied for the voter model on various networks [42–53]. For continuous-opinion models, perfect consensus would require an infinite amount of time, but one can define the convergence time to consensus in multiple reasonable manners. In particular, when a continuous-opinion dynamics is driven by an operator matrix, such as the Laplacian matrix, the convergence time has often been investigated in terms of the relevant eigenvalue of the matrix, such as the spectral gap of the Laplacian matrix [3,38,54–57]. However, these lines of research mainly focus on the dependence of the convergence time on the structure of the network of the same size rather than on that on the system size. The dependence of the consensus time on the system size in continuous-opinion models has been studied but mostly when the consensus is achievable in finite time, i.e., when interacting individuals end up having the same opinion, e.g., the average of their opinions as in some gossip models [58–60]. Therefore, the dependence of the convergence time on the system size in continuous-opinion models when the perfect consensus requires infinite time has not yet been thoroughly explored.

*h2jo@catholic.ac.kr

In the present study, we numerically investigate finite-size effects on the time towards consensus in a simple model of continuous-opinion dynamics without a bounded confidence, namely, the asymmetric-gossip model that was proposed in previous studies [3,40]. For this purpose, we consider networks with different numbers of nodes and structure. In the asymmetric-gossip model, a uniformly randomly chosen individual updates its opinion by partially mimicking the opinion of a uniformly randomly chosen neighbor. Thus, this model can be considered as a continuous-opinion version of the voter model.

II. MODEL

We study a continuous-opinion dynamics model proposed in Refs. [3,40]. In this model, which we refer to as the asymmetric-gossip model following Ref. [40], the opinion of each individual is represented by a real value. For a system of N individuals, we denote the opinion of the i th individual ($i = 1, \dots, N$) at time t by $x_i(t) \in [0, 1]$. The individuals interact on a connected network of N nodes, and an individual is located at each node. There are N attempts of opinion updating per unit time, which implies that each individual updates its opinion once per unit time on average. In each attempt of opinion updating, we first select an individual i with the equal probability, i.e., $1/N$, and then select one of i 's neighbors, say j , uniformly at random. Then, the i 's opinion approaches the j 's opinion depending on a learning rate parameter q ($0 \leq q \leq 1$) as follows:

$$x_i \left(t + \frac{1}{N} \right) = (1 - q)x_i(t) + qx_j(t), \tag{1}$$

which implies that the i 's new opinion is a weighted sum of the i 's old opinion and the j 's opinion. The j 's opinion remains the same.

If $q = 0$, the opinions never change over time. If $q = 1$, the model reduces to the multistate voter model [19,20]. When $q = 1$, in finite networks (i.e., $N < \infty$), the consensus in which all individuals share the same opinion is always reached in finite time. Finally, if $0 < q < 1$, the individuals are expected to converge to a single opinion, but in a manner different from that for the multistate voter model.

For describing the ordering dynamics of the individuals' continuous opinions when $0 < q < 1$, we measure the difference between the opinions of two neighboring individuals i and j at time t defined by

$$\rho_{ij}(t) \equiv |x_i(t) - x_j(t)|. \tag{2}$$

We define the network-level difference in opinion by

$$\rho(t) \equiv \frac{1}{|E|} \sum_{(i,j) \in E} \rho_{ij}(t), \tag{3}$$

where E is the set of edges of the network, and $|E|$ is the number of edges. In numerical simulations, we measure the convergence time, denoted by T , which we define as the time at which $\rho(t)$ becomes smaller than 10^{-10} for the first time.

In each simulation, we draw the initial opinion of each individual i uniformly randomly from the interval $[0,1]$.

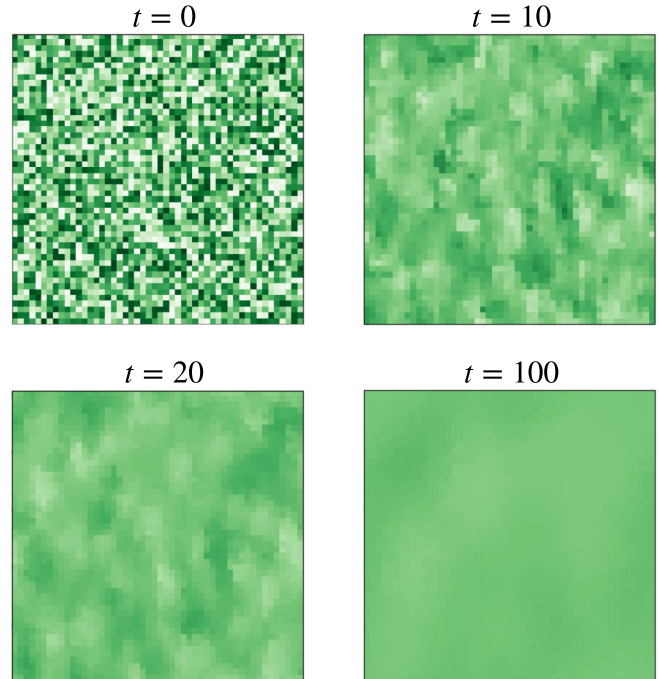


FIG. 1. Snapshots at different times of the dynamics of the asymmetric-gossip model on the two-dimensional lattice. We assume $N = 50 \times 50$ nodes and the periodic boundary conditions. We set $q = 1/2$. The opinion of a larger value is colored in a darker green. We implemented the visualization using the PyCX project [61].

III. RESULTS

A. Numerical results

We first numerically study the asymmetric-gossip model on finite-dimensional integer lattices with periodic boundary conditions, which we simply refer to as the lattice in the following text, random regular graphs (RRGs), and uncorrelated scale-free networks (SFNs).

1. Lattices

Let us consider the asymmetric-gossip model on the d -dimensional lattices with linear size L , combined with a periodic boundary condition. The network contains $N = L^d$ nodes. We show a typical time course of the model on the two-dimensional lattice with $q = 1/2$ in Fig. 1. We show the relationship between the convergence time, T , and L for $q = 1/2$ and $d = 1, \dots, 6$ in Fig. 2(a). The figure suggests the relationship $T \propto L^z$, where \propto denotes ‘‘proportional to.’’ Then, for each dimension d , we estimate the value of z by a linear fit between $\ln T$ and $\ln L$, as shown by the solid lines in Fig. 2(a). See Appendix A for details of the fitting procedure.

We show the estimated values of z by the solid line in Fig. 2(b). The figure suggests up to $d = 6$ that z slightly decreases from 2 as d increases. The deviation of z from 2 for higher d might be due to finite-size effects; for example, the largest linear size L in our numerical simulations is only 9 when $d = 6$. The z value being close to 2 can be related to the dynamic exponent for the normal diffusion (Appendix B). To later compare the present results with those for other networks, we define another exponent \bar{z} by

$$T \propto N^{\bar{z}}. \tag{4}$$

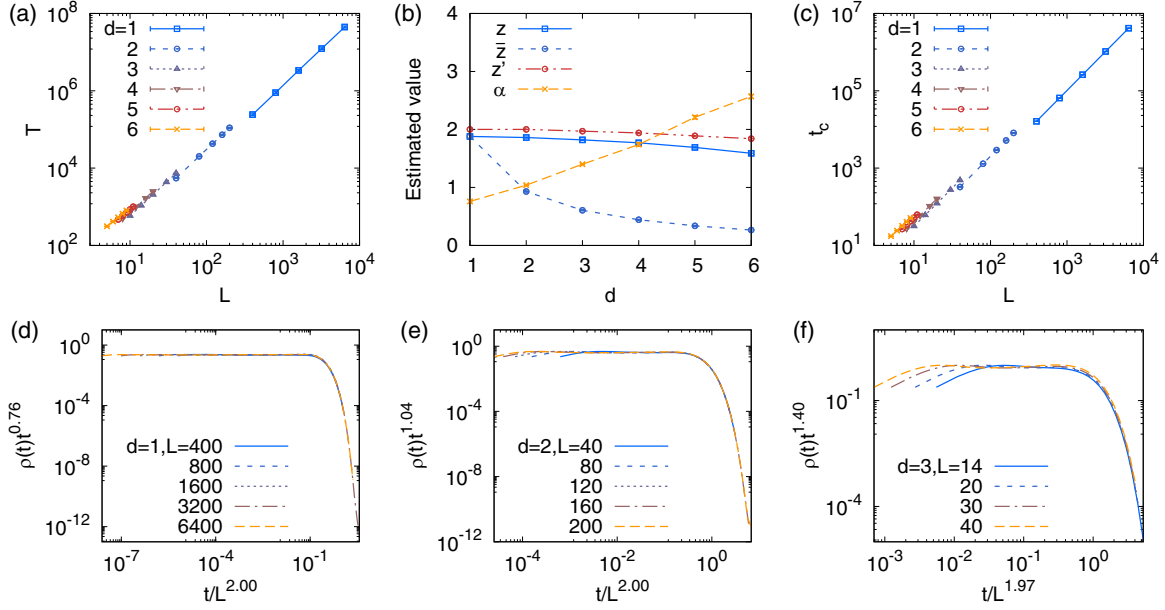


FIG. 2. Simulation results of the asymmetric-gossip model on d -dimensional lattices with $N = L^d$ nodes under periodic boundary conditions. We set $q = 1/2$. Each point or curve in panels (a), (d), (e), and (f) is an average over 100 simulations. We show the scaling behavior of T versus L for $d = 1, \dots, 6$ (a), the estimated values of z , \bar{z} , z' , and α , together with $\bar{z} = z/d$, for $d = 1, \dots, 6$ (b), the scaling behavior of t_c versus L for $d = 1, \dots, 6$ (c), and data collapse of $\rho(t)$ using the estimated values of z' and α for $d = 1$ (d), 2 (e), and 3 (f). In panels (a), (b), and (c), the error bars, representing the standard deviation, are smaller than the symbols.

Because $N = L^d$, one obtains

$$\bar{z} = \frac{z}{d}. \quad (5)$$

Exponent \bar{z} decreases as d increases [see Fig. 2(b)].

To further characterize dynamics towards convergence, we numerically examine $\rho(t)$ for the same variety of the values of d and L . In all cases $\rho(t)$ algebraically decays as a function of time before it starts to decay exponentially. Therefore, we assume that

$$\rho(t) \propto t^{-\alpha} e^{-t/t_c}, \quad t_c \propto L^{z'}, \quad (6)$$

where α is the decay exponent, and z' is the dynamic exponent relating the characteristic time t_c and the linear size L . Similar to the estimation of z , for each dimension d , we estimate the value of z' by a linear fit between $\ln t_c$ and $\ln L$ applied to the numerical results, as shown in Fig. 2(c). Then we estimate the value of α from $\rho(t)$ obtained for the largest value of L that we use. See Appendix A for details of the fitting procedure.

We show the estimated values of z' and α for $d = 1, \dots, 6$ in Fig. 2(b). The figure suggests up to $d = 6$ that α increases as d increases and that the behavior of z' is quantitatively similar to that of z . For each dimension, with the estimated values of z' and α , we find that the curves of $\rho(t)$ for different values of L collapse onto a single curve when we plot $\rho(t)t^\alpha$ versus $t/L^{z'}$, as shown in Figs. 2(d)–2(f).

We contrast these findings with the results for the voter model with two discrete opinions [62]. For the voter model, the density of edges connecting nodes with the opposite opinions, denoted by $\rho_a(t)$, decays as $\rho_a(t) \propto t^{-1/2}$ for $d = 1$, decays as $\rho_a(t) \propto (\ln t)^{-1}$ for $d = 2$, and converges to a positive constant for $d > 2$. The consensus time, denoted by \bar{T} , for the voter model in finite networks scales as $\bar{T} \propto N^2$ for $d = 1$,

$\bar{T} \propto N \ln N$ for $d = 2$, and $\bar{T} \propto N$ for $d > 2$, implying that $\bar{z} = 2$ for $d = 1$ and $\bar{z} = 1$ for $d \geq 2$. The mean-field theory for the original and multistate voter models in finite networks also yields $\bar{z} = 1$ [19,51]. The numerically estimated values of \bar{z} for the asymmetric-gossip model and the result for the voter model are consistent with each other for $d \leq 2$, but they are different for $d > 2$. We also remark that the Ising model and a variant of the voter model called the confident voter model on two-dimensional lattices often show the metastable structure (e.g., stripes) that induces two different timescales for relaxation; see Refs. [63,64] for the Ising model and Ref. [65] for the confident voter model. The present asymmetric-gossip model does not show such metastable states.

2. Regular random graphs

Next, we perform the numerical simulations of the asymmetric-gossip model on the RRGs. The numerical results in the case of $q = 1/2$ and the node's degree $k = 4, 8$, and 16 are shown in Figs. 3(a), 3(b), and 3(c), respectively. We find that $\rho(t)$ is independent of N for each k value. Therefore, T is independent of N , i.e., $\bar{z} = 0$ [see Fig. 3(d)]. As is the case for various complex networks, RRGs are considered to have $d \rightarrow \infty$. Therefore, the result that $\bar{z} = 0$ is consistent with that for the lattices, for which \bar{z} decreases as the dimension of the lattice, d , increases, roughly according to $\bar{z} \approx 2/d$ [see Fig. 2(b)]. Our result that $\bar{z} = 0$ is again different from the known result for the voter model on uncorrelated networks including RRGs, i.e., $\bar{z} = 1$ [51].

3. Scale-free networks

In this section, we study the asymmetric-gossip model on the uncorrelated SFNs. We assume that the node's degree

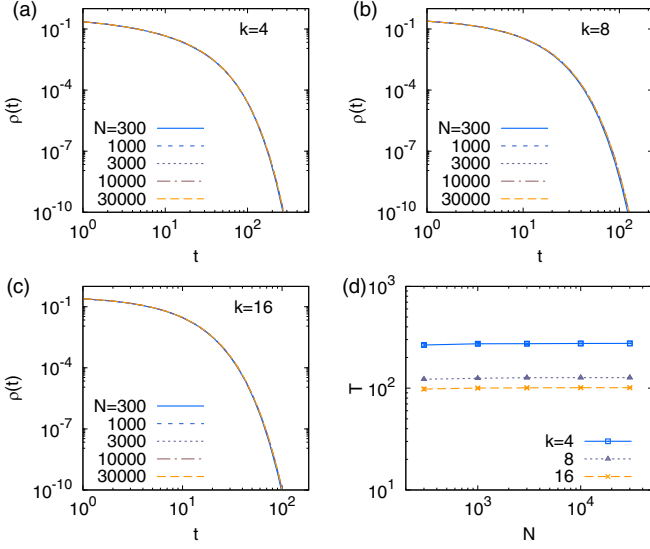


FIG. 3. Simulation results of the asymmetric-gossip model on random regular graphs (RRGs) with N nodes and degree k for each node. We set $q = 1/2$. Each point on the curve is an average over 100 simulations on a single realization of the RRG. We show $\rho(t)$ for various network sizes with $k = 4$ (a), 8 (b), and 16 (c). The convergence time is plotted in panel (d), where the error bars represent the standard deviation.

obeys a power-law distribution given by $P(k) = Ck^{-\gamma}$ for $k \geq k_{\min} = 2$ with the degree exponent γ and normalization constant C . We generate the SFNs based on the uncorrelated configuration model [66]. In other words, we begin with N isolated nodes to each of which we assign degree k_i (for $i = 1, \dots, N$) that is drawn from the distribution $P(k)$. Then, conditioned that $\sum_{i=1}^N k_i$ is an even number, we select a pair of nodes with probabilities proportional to their remaining degrees, i.e., k_i subtracted by the present degree, and connect them by an edge if both of their current degrees are smaller than the assigned degrees and there is no edge between them. We repeat this wiring procedure until all nodes have the actual degree k_i . In practice, we terminate the wiring procedure when nodes with positive remaining degrees are already connected to each other or when there is only one node with the positive remaining degree. The generated networks are connected.

The numerical results on SFNs are shown in Fig. 4 for $q = 1/2$ and for several values of γ and N . We find that both $\rho(t)$ and T are only slightly affected by N , which implies that $\bar{z} \approx 0$, for a range of γ .

For the voter model on SFNs, the consensus time scales as $\bar{T} \propto N$ for $\gamma > 3$, $\bar{T} \propto N/\ln N$ for $\gamma = 3$, $\bar{T} \propto N^{(2\gamma-4)/(\gamma-1)}$ for $2 < \gamma < 3$, $\bar{T} \propto (\ln N)^2$ for $\gamma = 2$, and $\bar{T} \propto O(1)$ for $\gamma < 2$ [45]. Therefore, \bar{z} is dependent on γ and positive for the voter model if $\gamma > 2$. In contrast, we obtain $\bar{z} \approx 0$ for any $\gamma \geq 2.5$ in the asymmetric-gossip model.

4. Effect of the learning rate parameter q

We now study the effect of the learning rate parameter q , introduced in Eq. (1). We show the convergence time, T , as a function of q for the lattices, RRGs, and SFNs of different sizes in Fig. 5. In all cases, we find the optimal value of q

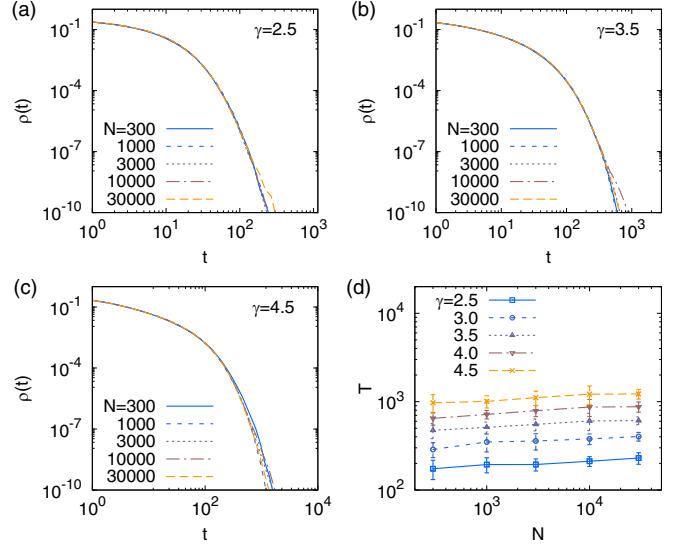


FIG. 4. Simulation results of the asymmetric-gossip model on uncorrelated scale-free networks (SFNs) with degree distribution $P(k) \propto k^{-\gamma}$. We set $q = 1/2$. Each point on the curve is an average over 100 simulations. For each pair of the N and γ values, we generate 50 SFNs to perform two simulations on each of them. We show $\rho(t)$ for various network sizes with $\gamma = 2.5$ (a), 3.5 (b), and 4.5 (c). The convergence time is plotted in panel (d), where the error bars represent the standard deviation.

between 0 and 1 in terms of the convergence speed, making T the smallest. These results imply that the faster learning does not always speed up the convergence.

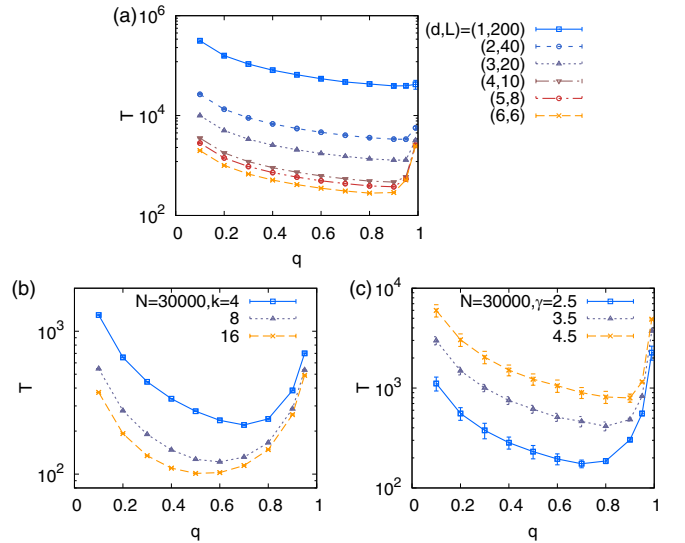


FIG. 5. Convergence time, T , of the asymmetric-gossip model on the different networks as a function of q . (a) d -dimensional lattices with linear size L . (b) Regular random graphs with degree k . (c) Uncorrelated scale-free networks with degree exponent γ . These networks are the same as those used in Figs. 2–4. Each symbol is an average over 100 simulations. The error bars represent the standard deviation.

B. Mean-field analysis

To understand our numerical results, in this section we analyze the mean-field case where every node equally interacts with every other node. The state of the system at time t is specified by the distribution of opinions, $\{x_i(t)\}$, which we denote by $P_t(x)$. By using Eq. (1) and approximating the original discrete time by continuous time, which corresponds to the limit $N \rightarrow \infty$, we obtain the following master equation to describe the dynamics of $P_t(x)$:

$$\frac{\partial P_t(x)}{\partial t} = \int_0^1 dx_i \int_0^1 dx_j P_t(x_i) P_t(x_j) \times [\delta(x - (1-q)x_i - qx_j) - \delta(x - x_i)], \quad (7)$$

where δ denotes Dirac delta. In Eq. (7), x_i and x_j are the opinions of a uniformly randomly chosen node i , whose opinion changes at time t , and another uniformly randomly chosen node j , respectively. Equation (7) is similar to the equation that has originally been proposed for representing inelastic collisions of particles [67,68]. By taking the Laplace transform of Eq. (7) with respect to x over the range $[0,1]$, one obtains

$$\frac{\partial \tilde{P}_t(s)}{\partial t} = -\tilde{P}_t(s) + \tilde{P}_t((1-q)s)\tilde{P}_t(qs), \quad (8)$$

where

$$\tilde{P}_t(s) \equiv \int_0^1 dx e^{-xs} P_t(x). \quad (9)$$

We expand the exponential term in Eq. (9) to obtain

$$\tilde{P}_t(s) = \sum_{n=0}^{\infty} \frac{(-s)^n}{n!} c_n(t), \quad (10)$$

where

$$c_n(t) \equiv \int_0^1 dx x^n P_t(x) \quad (11)$$

is the n th moment of x at time t . Note that $c_0(t) = 1$ for any t . The initial uniform distribution of the opinions implies $P_0(x) = 1$ for $x \in [0, 1]$, which translates into $c_1(0) = 1/2$. By plugging Eq. (10) into Eq. (8) and comparing the coefficients of s and s^2 , we obtain

$$\frac{dc_1(t)}{dt} = 0, \quad (12)$$

$$\frac{dc_2(t)}{dt} = -2q(1-q)c_2(t) + \frac{q(1-q)}{2}. \quad (13)$$

For the second equation, we have used the fact that $c_1(t) = c_1(0) = 1/2$.

Instead of using $\rho(t)$ given by Eq. (3), one can also describe the ordering dynamics in terms of the temporal evolution of the variance of opinions, i.e.,

$$\begin{aligned} v(t) &\equiv \langle x(t)^2 \rangle - \langle x(t) \rangle^2 \\ &= c_2(t) - c_1(t)^2 \\ &= c_2(t) - \frac{1}{4}. \end{aligned} \quad (14)$$

By substituting Eq. (14) into Eq. (13), we obtain

$$\frac{dv(t)}{dt} = -2q(1-q)v(t). \quad (15)$$

Therefore, for $0 < q < 1$ we obtain

$$v(t) = v(0)e^{-t/\tau_c}, \quad (16)$$

where

$$\tau_c \equiv \frac{1}{2q(1-q)}. \quad (17)$$

Therefore, the opinion distribution, $P_t(x)$, converges to $\delta(x - 1/2)$, i.e., the consensus at $x = 1/2$, exponentially fast. Equation (17) implies that the convergence time, T , is also proportional to $[q(1-q)]^{-1}$, which we numerically confirm for complete graphs [see Fig. 6(a)]. Note that the convergence time, T , for the complete graph is independent of the number of nodes, N , for $q = 0.1, \dots, 0.9$, which we used in Fig. 6(a).

C. Crossover behavior

We have found for RRGs and SFNs that $\bar{z} \approx 0$ for $0 < q < 1$. However, we expect to find $\bar{z} = 1$, i.e., $T \propto N$ for $q = 1$ because when $q = 1$, the asymmetric-gossip model reduces to the multistate voter model. Therefore, we expect to find a crossover between the $q < 1$ regime and the $q = 1$ case in terms of the dependence of T on N . To study this crossover behavior, we carry out numerical simulations on the complete graph with several values of q close to one.

We show the relationship between T and N in Fig. 6(b). The figure suggests for each q that $T \propto N$ for $N \ll N_\times$ and that T is constant for $N \gg N_\times$, where N_\times denotes a crossover system size. Therefore, we assume that

$$T = T_\infty f\left(\frac{N}{N_\times}\right), \quad (18)$$

where

$$f(r) = \begin{cases} r & \text{if } r \ll 1, \\ 1 & \text{if } r \gg 1. \end{cases} \quad (19)$$

Note that N_\times may depend on q . If $N \gg N_\times$, one obtains $T = T_\infty$, which implies that T_∞ is the convergence time for large N . In Sec. III B we suggested $T_\infty \propto [q(1-q)]^{-1}$ based on the mean-field theory. Therefore, we assume that $T_\infty = a/[q(1-q)]$ with $a = 21.8$ [see also Fig. 6(a)]. If $N \ll N_\times$, then Eqs. (18) and (19) imply that $T = (T_\infty/N_\times)N \equiv bN$. We estimate $b = 3.55$ by the linear fit between T and N using numerical results obtained for $N = 100, \dots, 1600$ with $q = 0.999$. Then we write N_\times as follows:

$$N_\times = \frac{T_\infty}{b} = \frac{a}{bq(1-q)}. \quad (20)$$

Consequently, as q approaches one, N_\times diverges. Using these T_∞ and N_\times values, which depend on q , we plot T/T_∞ as a function of N/N_\times for various values of q in Fig. 6(c). We find that all curves roughly collapse onto a single curve that satisfies Eq. (19).

We remark that the crossover behavior between different N -dependences of the consensus time \bar{T} has been reported for other opinion dynamics models with discrete opinions: $\bar{T} \propto N^{1.6}$ for $N < N_\times$ and $\bar{T} \propto N^{0.2}$ for $N > N_\times$ on the one-dimensional lattice, and $\bar{T} \propto N^{0.6}$ for $N < N_\times$ and $\bar{T} \propto N^{0.1}$ for $N > N_\times$ on the two-dimensional lattice [69,70].

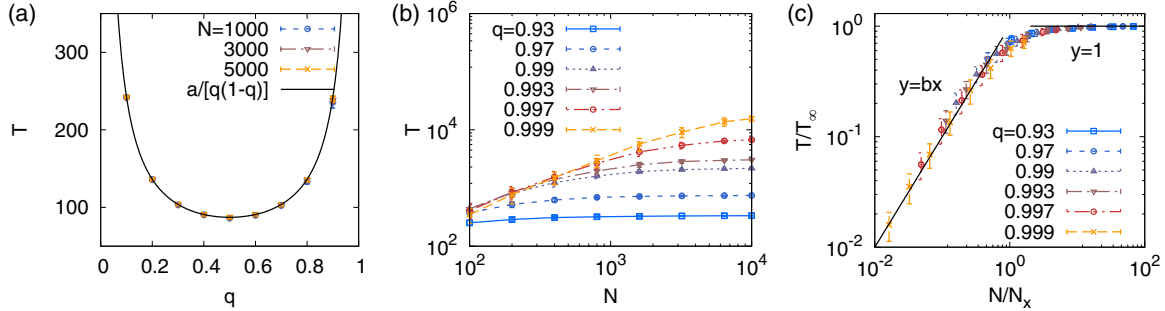


FIG. 6. Convergence time for the asymmetric-gossip model on complete graphs. Each symbol is an average over 100 simulations. (a) Convergence time, T , as a function of q for $N = 10^3$, 3×10^3 , and 5×10^3 . The solid curve represents the analytical form of T , i.e., $a/[q(1 - q)]$, where a is a constant, which we set to 21.8; see Eq. (17). (b) Convergence time as a function of N for various values of q close to 1. (c) Data collapse of T/T_∞ as a function of N/N_x based on the results shown in panel (b). We set $T_\infty = a/[q(1 - q)]$ and $N_x = T_\infty/b$, where $b = 3.55$. In all panels, the error bars represent the standard deviation. The solid lines in (c) represent $y = 1$ and $y = bx$.

IV. CONCLUSION

We have studied an asymmetric-gossip model for continuous-opinion dynamics without a bounded confidence. We have specifically focused on the effects of the system size, N , i.e., the number of individuals, on the convergence time, T . We numerically find that the scaling exponent relating T and N depends on the dimension of the lattices. In contrast, T is approximately independent of N for the regular random graphs, uncorrelated scale-free networks, and complete graphs. We have presented a mean-field analysis to support the numerical results for the complete graphs.

In Ref. [55] the authors analyzed the convergence time of a model similar to the present asymmetric-gossip model. Their model is a broadcast asymmetric-gossip model. In other words, when a node i updates its state according to Eq. (1), all the nodes adjacent to node j do so at the same time such that j broadcasts its opinion to all its neighbors. They considered spatial networks to find that there is a value of q , where $0 < q < 1$, which minimizes the convergence time. This result is consistent with our numerical results for the lattices, RRGs, and SFNs [see Fig. 5] and our theoretical result that the convergence is the fastest at $q = 1/2$ on the complete graph [see Eq. (17)]. Future questions in this direction include how our scaling results extend to broadcast gossip models, how the optimal q values depend on the network structure, and how we can leverage linear algebra techniques [40,55] to further understand the present asymmetric-gossip model.

As future work, it may also be interesting to study finite-size effects on the convergence time in more complicated, realistic models with continuous opinions, such as mul-

tidimensional Deffuant-Weisbuch and Hegselmann-Krause models [4,71,72].

ACKNOWLEDGMENTS

H.-H.J. thanks J. D. Noh for fruitful comments on the initial draft and acknowledges financial support by Basic Science Research Program through the National Research Foundation of Korea (NRF) grant funded by the Ministry of Education (NRF-2018R1D1A1A09081919) and by the Catholic University of Korea, Research Fund, 2020. N.M. acknowledges support from AFOSR European Office (under Grant No. FA9550-19-1-7024), the Nakatani Foundation, and the Sumitomo Foundation.

APPENDIX A: ESTIMATION OF z, z' , AND α VALUES FOR LATTICES

On the lattice of each dimension, d , and each linear size, L , shown in Table I, we run 100 simulations with different initial conditions to obtain the average convergence time T as well as the average curve of $\rho(t)$. Then we estimate the value of z by the linear fit between $\ln T$ and $\ln L$, which is informed by the assumption that $T \propto L^z$. The estimated values of z and their standard errors are shown in the third column of Table I.

From $\rho(t)$, we estimate t_c by the linear fit between $\ln \rho(t)$ and t for a range of t showing the exponentially decaying behavior. We show the range of t used for the fitting in each case in the fourth column of Table I. Once the values of t_c for all the values of L considered are ready, we estimate the value of z' by the linear fit between $\ln t_c$ and $\ln L$, which is informed

TABLE I. Details of the simulation on lattices and the estimation of z, z' , and α values. For each dimension d , we show the linear sizes L , estimated value of z with standard error in parentheses, fitting ranges of t for t_c , estimated value of z' with standard error in parentheses, fitting range of t for α , and estimated value of α with the standard error in parentheses.

d	L	z	Fitting range of t for t_c	z'	Fitting range of t for α	α
1	400,800,1600,3200,6400	1.88(1)	$\geq 2 \times 10^4, \geq 8 \times 10^4, \geq 2 \times 10^5, [10^6, 3 \times 10^7], \geq 5 \times 10^6$	2.00(1)	$[e^{2.5}, e^{15}]$	0.76(1)
2	40,80,120,160,200	1.86(1)	$\geq 500, \geq 2000, \geq 5000, [10^4 : 14 \times 10^4], [2 \times 10^4 : 25 \times 10^4]$	2.00(1)	$[e^{2.5}, e^9]$	1.04(1)
3	10,14,20,30,40	1.82(1)	$\geq 70, \geq 150, \geq 300, \geq 500, \geq 1000$	1.97(1)	$[e^{2.5}, e^6]$	1.40(1)
4	8,10,12,16,20	1.77(1)	$\geq 80, \geq 100, \geq 180, \geq 250, \geq 300$	1.94(1)	$[e^{2.5}, e^{5.5}]$	1.74(3)
5	7,8,9,10,11	1.69(1)	$\geq 60, \geq 70, \geq 90, \geq 100, \geq 150$	1.89(1)	$[e^{2.5}, e^5]$	2.21(3)
6	5,6,7,8,9	1.59(2)	$\geq 50, \geq 80, \geq 90, \geq 100, \geq 120$	1.84(2)	$[e^{2.5}, e^5]$	2.57(4)

by the assumption that $t_c \propto L^z$. The estimated values of z' and their standard errors are shown in the fifth column of Table I.

As mentioned in the main text, for each d , we compute the value of α from the $\rho(t)$ for the largest L . We estimate the value of α by the linear fit between $\ln \rho(t)$ and $\ln t$ for a range of t showing the scaling behavior, which is listed in the sixth column of Table I. The estimated values of α with their standard errors are shown in the seventh column of Table I.

APPENDIX B: RELATION OF THE ASYMMETRIC-GOSSIP MODEL TO THE DIFFUSION PROCESS

We can interpret the update rule in Eq. (1) as a normal diffusion process. To show this, we expand the left-hand side of Eq. (1) assuming $N \gg 1$ to obtain

$$\frac{dx_i(t)}{dt} = Nq[x_j(t) - x_i(t)]. \quad (\text{B1})$$

On one-dimensional lattices, j is either $i - 1$ or $i + 1$ with probability $1/2$ each. Therefore, the expectation of $x_i(t)$, denoted by $E[x_i(t)]$, evolves according to

$$\frac{dE[x_i(t)]}{dt} = \frac{Nq}{2}\{E[x_{i-1}(t)] + E[x_{i+1}(t)] - 2E[x_i(t)]\}. \quad (\text{B2})$$

One can approximate Eq. (B2) in the continuous space by the normal diffusion equation as follows:

$$\frac{dE[x(y, t)]}{dt} \approx D \frac{d^2 E[x(y, t)]}{dy^2}, \quad (\text{B3})$$

with a diffusion constant $D = Nq/2$, where \approx represents “approximately equal to”. The dynamic exponent z relating the timescale and the length scale of the normal diffusion given by Eq. (B3) is 2. The same derivation applies to the higher-dimensional lattices with a dimension-dependent diffusion constant $D = Nq/(2d)$, where we remind that d is the dimension.

-
- [1] C. Castellano, S. Fortunato, and V. Loreto, Statistical physics of social dynamics, *Rev. Mod. Phys.* **81**, 591 (2009).
- [2] P. Sen and B. K. Chakrabarti, *Sociophysics: An Introduction* (Oxford University Press, Oxford, 2014).
- [3] D. Acemoglu and A. Ozdaglar, Opinion dynamics and learning in social networks, *Dyn. Games Appl.* **1**, 3 (2011).
- [4] A. Sírbu, V. Loreto, V. D. P. Servedio, and F. Tria, Opinion dynamics: Models, extensions and external effects, in *Participatory Sensing, Opinions and Collective Awareness*, edited by V. Loreto, M. Haklay, A. Hotho, V. D. Servedio, G. Stumme, J. Theunis, and F. Tria (Springer International Publishing, Cham, 2017), pp. 363–401.
- [5] A. V. Proskurnikov and R. Tempo, A tutorial on modeling and analysis of dynamic social networks. Part I, *Annu. Rev. Control* **43**, 65 (2017).
- [6] A. V. Proskurnikov and R. Tempo, A tutorial on modeling and analysis of dynamic social networks. Part II, *Annu. Rev. Control* **45**, 166 (2018).
- [7] A. Baronchelli, The emergence of consensus: A primer, *R. Soc. Open Sci.* **5**, 172189 (2018).
- [8] B. D. O. Anderson and M. Ye, Recent advances in the modelling and analysis of opinion dynamics on influence networks, *Int. J. Automat. Comput.* **16**, 129 (2019).
- [9] H. Noorazar, Recent advances in opinion propagation dynamics: A 2020 survey, *Eur. Phys. J. Plus* **135**, 521 (2020).
- [10] S. P. Borgatti, A. Mehra, D. J. Brass, and G. Labianca, Network analysis in the social sciences, *Science* **323**, 892 (2009).
- [11] A.-L. Barabási and M. Pósfai, *Network Science* (Cambridge University Press, Cambridge, 2016).
- [12] M. E. J. Newman, *Networks*, 2nd ed. (Oxford University Press, Oxford, 2018).
- [13] F. Menczer, S. Fortunato, and C. A. Davis, *A First Course in Network Science* (Cambridge University Press, Cambridge, 2020).
- [14] P. Clifford and A. Sudbury, A model for spatial conflict, *Biometrika* **60**, 581 (1973).
- [15] R. A. Holley and T. M. Liggett, Ergodic theorems for weakly interacting infinite systems and the voter model, *Ann. Probab.* **3**, 643 (1975).
- [16] T. M. Liggett, *Stochastic Interacting Systems: Contact, Voter and Exclusion Processes*, Grundlehren der mathematischen Wissenschaften, Vol. 324 (Springer, Berlin, 1999).
- [17] S. Redner, Reality-inspired voter models: A mini-review, *C. R. Phys.* **20**, 275 (2019).
- [18] M. Howard and C. Godrèche, Persistence in the Voter model: Continuum reaction-diffusion approach, *J. Phys. A: Math. Gen.* **31**, L209 (1998).
- [19] M. Starnini, A. Baronchelli, and R. Pastor-Satorras, Ordering dynamics of the multi-state voter model, *J. Stat. Mech.: Theory Exp.* (2012) P10027.
- [20] W. Pickering and C. Lim, Solution of the multistate voter model and application to strong neutrals in the naming game, *Phys. Rev. E* **93**, 032318 (2016).
- [21] F. Vazquez, E. S. Loscar, and G. Baglietto, Multistate voter model with imperfect copying, *Phys. Rev. E* **100**, 042301 (2019).
- [22] P. Holme and M. E. J. Newman, Nonequilibrium phase transition in the coevolution of networks and opinions, *Phys. Rev. E* **74**, 056108 (2006).
- [23] D. Kimura and Y. Hayakawa, Coevolutionary networks with homophily and heterophily, *Phys. Rev. E* **78**, 016103 (2008).
- [24] J. L. Herrera, M. G. Cosenza, K. Tucci, and J. C. González-Avella, General coevolution of topology and dynamics in networks, *EPL (Europhys. Lett.)* **95**, 58006 (2011).
- [25] G. A. Böhme and T. Gross, Fragmentation transitions in multi-state voter models, *Phys. Rev. E* **85**, 066117 (2012).
- [26] A. Brunstein and T. Tomé, Universal behavior in an irreversible model with C3v symmetry, *Phys. Rev. E* **60**, 3666 (1999).
- [27] T. Tome and A. Petri, Cumulants of the three-state Potts model and of nonequilibrium models with C3v symmetry, *J. Phys. A: Math. Gen.* **35**, 5379 (2002).

- [28] P. Chen and S. Redner, Consensus formation in multi-state majority and plurality models, *J. Phys. A: Math. Gen.* **38**, 7239 (2005).
- [29] D. F. F. Melo, L. F. C. Pereira, and F. G. B. Moreira, The phase diagram and critical behavior of the three-state majority-vote model, *J. Stat. Mech.: Theory Exp.* (2010) P11032.
- [30] G. Li, H. Chen, F. Huang, and C. Shen, Discontinuous phase transition in an annealed multi-state majority-vote model, *J. Stat. Mech.: Theory Exp.* (2016) 073403.
- [31] H. Chen and G. Li, Phase transitions in a multistate majority-vote model on complex networks, *Phys. Rev. E* **97**, 062304 (2018).
- [32] G. Deffuant, D. Neau, F. Amblard, and G. Weisbuch, Mixing beliefs among interacting agents, *Adv. Complex Syst.* **03**, 87 (2000).
- [33] R. Hegselmann and U. Krause, Opinion dynamics and bounded confidence: Models, analysis and simulation, *J. Artif. Soc. Social Simul.* **5**, 2 (2002).
- [34] J. Lorenz, Continuous opinion dynamics under bounded confidence: A survey, *Int. J. Mod. Phys. C* **18**, 1819 (2007).
- [35] R. Abelson, Mathematical models of the distribution of attitudes under controversy, in *Contributions to Mathematical Psychology*, edited by N. Frederiksen and H. Gulliksen (Rinehart Winston, New York, 1964), pp. 142–160.
- [36] M. H. DeGroot, Reaching a consensus, *J. Am. Stat. Assoc.* **69**, 118 (1974).
- [37] N. E. Friedkin and E. C. Johnsen, Social influence and opinions, *J. Math. Sociol.* **15**, 193 (1990).
- [38] S. Boyd, A. Ghosh, B. Prabhakar, and D. Shah, Randomized gossip algorithms, *IEEE Trans. Inf. Theory* **52**, 2508 (2006).
- [39] R. Olfati-Saber, J. A. Fax, and R. M. Murray, Consensus and cooperation in networked multi-agent systems, *Proc. IEEE* **95**, 215 (2007).
- [40] F. Fagnani and S. Zampieri, Randomized consensus algorithms over large scale networks, *IEEE J. Sel. Areas Commun.* **26**, 634 (2008).
- [41] C. Nowzari, E. Garcia, and J. Cortés, Event-triggered communication and control of networked systems for multi-agent consensus, *Automatica* **105**, 1 (2019).
- [42] J. T. Cox, Coalescing random walks and voter model consensus times on the torus in Zd, *Ann. Probab.* **17**, 1333 (1989).
- [43] D. ben-Abraham, D. Considine, P. Meakin, S. Redner, and H. Takayasu, Saturation transition in a monomer-monomer model of heterogeneous catalysis, *J. Phys. A: Math. Gen.* **23**, 4297 (1990).
- [44] D. Vilone and C. Castellano, Solution of voter model dynamics on annealed small-world networks, *Phys. Rev. E* **69**, 016109 (2004).
- [45] V. Sood and S. Redner, Voter Model on Heterogeneous Graphs, *Phys. Rev. Lett.* **94**, 178701 (2005).
- [46] K. Suchecki, V. M. Eguíluz, and M. S. Miguel, Voter model dynamics in complex networks: Role of dimensionality, disorder, and degree distribution, *Phys. Rev. E* **72**, 036132 (2005).
- [47] K. Suchecki, V. M. Eguíluz, and M. S. Miguel, Conservation laws for the voter model in complex networks, *Europhys. Lett. (EPL)* **69**, 228 (2005).
- [48] C. Castellano, V. Loreto, A. Barrat, F. Cecconi, and D. Parisi, Comparison of voter and Glauber ordering dynamics on networks, *Phys. Rev. E* **71**, 066107 (2005).
- [49] C. Castellano, Effect of network topology on the ordering dynamics of voter models, in *AIP Conference Proceedings*, Vol. 779 (AIP, Granada, Spain, 2005), pp. 114–120, <https://aip.scitation.org/action/showCitFormats?type=show&doi=10.1063%2F1.2008600>.
- [50] V. Sood, T. Antal, and S. Redner, Voter models on heterogeneous networks, *Phys. Rev. E* **77**, 041121 (2008).
- [51] F. Vazquez and V. M. Eguíluz, Analytical solution of the voter model on uncorrelated networks, *New J. Phys.* **10**, 063011 (2008).
- [52] Y. Iwamasa and N. Masuda, Networks maximizing the consensus time of voter models, *Phys. Rev. E* **90**, 012816 (2014).
- [53] N. Masuda, Voter model on the two-clique graph, *Phys. Rev. E* **90**, 012802 (2014).
- [54] J. A. Almendral and A. Díaz-Guilera, Dynamical and spectral properties of complex networks, *New J. Phys.* **9**, 187 (2007).
- [55] T. Aysal, M. Yildiz, A. Sarwate, and A. Scaglione, Broadcast gossip algorithms for consensus, *IEEE Trans. Signal Proc.* **57**, 2748 (2009).
- [56] N. Masuda, K. Klemm, and V. M. Eguíluz, Temporal Networks: Slowing Down Diffusion by Long Lasting Interactions, *Phys. Rev. Lett.* **111**, 188701 (2013).
- [57] Z. Chen, L. Cai, and C. Zhao, Convergence time of average consensus with heterogeneous random link failures, *Automatica* **127**, 109496 (2021).
- [58] G. Shi, B. Li, M. Johansson, and K. H. Johansson, Finite-time convergent gossiping, *IEEE/ACM Trans. Netw.* **24**, 2782 (2016).
- [59] M. M. Aiyad and G. Di Fatta, Agreement in epidemic data aggregation, in *2017 IEEE 23rd International Conference on Parallel and Distributed Systems (ICPADS)* (IEEE, Shenzhen, 2017), pp. 738–746.
- [60] S. Kouachi, S. Dhuli, and Y. N. Singh, Convergence rate analysis of periodic gossip algorithms for one-dimensional lattice WSNs, *IEEE Sens. J.* **20**, 13150 (2020).
- [61] H. Sayama, PyCX: A Python-based simulation code repository for complex systems education, *Complex Adapt. Syst. Model.* **1**, 2 (2013).
- [62] P. L. Krapivsky, S. Redner, and E. Ben-Naim, *A Kinetic View of Statistical Physics* (Cambridge University Press, Cambridge, 2010).
- [63] V. Spirin, P. L. Krapivsky, and S. Redner, Fate of zero-temperature Ising ferromagnets, *Phys. Rev. E* **63**, 036118 (2001).
- [64] V. Spirin, P. L. Krapivsky, and S. Redner, Freezing in Ising ferromagnets, *Phys. Rev. E* **65**, 016119 (2001).
- [65] D. Volovik and S. Redner, Dynamics of confident voting, *J. Stat. Mech.: Theory Exp.* (2012) P04003.
- [66] M. Catanzaro, M. Boguñá, and R. Pastor-Satorras, Generation of uncorrelated random scale-free networks, *Phys. Rev. E* **71**, 027103 (2005).
- [67] E. Ben-Naim, P. Krapivsky, and S. Redner, Bifurcations and patterns in compromise processes, *Physica D* **183**, 190 (2003).
- [68] E. Ben-Naim and P. L. Krapivsky, Multiscaling in inelastic collisions, *Phys. Rev. E* **61**, R5(R) (2000).
- [69] C. J. Tessone, R. Toral, P. Amengual, H. S. Wio, and M. San Miguel, Neighborhood models of minority opinion spreading, *Eur. Phys. J. B* **39**, 535 (2004).
- [70] R. Toral and C. J. Tessone, Finite size effects in the dynamics of opinion formation, *Commun. Comput. Phys.* **2**, 177 (2007).

- [71] S. Fortunato, V. Latora, A. Pluchino, and A. Rapisarda, Vector opinion dynamics in a bounded confidence consensus model, [Int. J. Mod. Phys. C](#) **16**, 1535 (2005).
- [72] J. Lorenz, Continuous opinion dynamics of multidimensional allocation problems under bounded confidence. More dimensions lead to better chances for consensus, [Eur. J. Econ. Social Syst.](#) **19**, 213 (2006).